J. Fluid Mech. (1995), *vol.* 284, *pp.* 159–169

Boundary layer flow of air over water on a flat plate

By JOHN J. NELSON[1], AMY E. ALVING[2] AND DANIEL D. JOSEPH[2,3]

[1] United States Air Force Wright Laboratories, Wright-Patterson Air Force Base, OH 45433-7913, USA

[2] Department of Aerospace Engineering and Mechanics, University of Minnesota, 110 Union Street, S.E., Minneapolis, MN 55455, USA

[3] The Minnesota Supercomputer Institute, University of Minnesota, 110 Union Street, S.E., Minneapolis, MN 55455, USA

(Received 28 July 1993 and in revised form 25 August 1994)

A non-similar boundary layer theory for air blowing over a water layer on a flat plate is formulated and studied as a two-fluid problem in which the position of the interface is unknown. The problem is considered at large Reynolds number (based on x), away from the leading edge. We derive a simple non-similar analytic solution of the problem for which the interface height is proportional to $x^{1/4}$ and the water and air flow satisfy the Blasius boundary layer equations, with a linear profile in the water and a Blasius profile in the air. Numerical studies of the initial value problem suggest that this asymptotic non-similar air–water boundary layer solution is a global attractor for all initial conditions.

1. Introduction

The effects of water layers driven over solid surfaces by wind are of interest in the performance of aircraft in rain, for the de-icing of airplane wings and surely in many other applications. Since such problems are intrinsically of a boundary layer type and since the more interesting phenomenon which might arise, like the formation of waves, film rupture and the like are probably best framed in terms of stability, it is necessary to derive the analytic forms that such flows will take when instability is neglected. This derivation is carried out here.

Previous works related to the present one are by Yih (1990), who modelled the de-icing problem, and by Wang (1992), who considered the development of boundary layers in the shearing flow of one fluid over another. Both works are flawed by assuming rather than finding the shape of the interface. In the case treated by Wang, the interface is flat but the jump of the normal stress is not zero. Yih assumed that the flow in the air is a Blasius flow and the flow in the water is a simple shear. This is a correct form for the boundary layer, as we shall show, but he neglects the variation of film thickness with x and so cannot enforce the kinematic condition at the interface or find its shape.

In this work, we formulate a non-similar boundary layer theory retaining all terms which decay slower than $1/\xi, \xi = x(U/2\nu_2 x)^{1/2}$, where ν_2 is the kinematic viscosity of air. All of the interface conditions are enforced in this asymptotic regime. An effect of the small but non-zero vertical velocity component at the interface is to force the interface to grow like $x^{1/4}$ when the boundary layer in the air grows like $x^{1/2}$. The

interface looks thin on the scale of the boundary layer. Asymptotically, at large x, the water and air satisfy the Blasius boundary layer equations with a linear profile in the water and the flat plate profile in the air. This non-similar (or coupled self-similar) solution appears to be a global attractor for all initial conditions.

2. Governing equations

A water film of height $y = h(x)$ is flowing on a flat plate. Shear stress is exerted on the water by an air stream of velocity U flowing above the water layer, $y > h(x)$. The volume flow rate in the water layer is specified to be Q. We seek the nature of the flow under the circumstances which give rise to Blasius boundary layers in the flow of one fluid over a flat plate. This motivates the introduction of the same scales that are used in the classical case, giving

$$\left.\begin{aligned} &\xi = \left(\frac{Ux}{2\nu_2}\right)^{1/2}, \quad \eta = y\left(\frac{U}{2\nu_2 x}\right)^{1/2}, \quad \eta^* = h(x)\left(\frac{U}{2\nu_2 x}\right)^{1/2}, \quad u = \frac{u}{U}, \\ &v = v\left(\frac{2x}{U\nu_2}\right)^{1/2}, \quad \tau = \frac{tU^2}{\nu_2}, \quad p = \frac{p}{\rho_2 U^2}, \quad f = \frac{\psi}{(2\nu_2 xU)^{1/2}}, \end{aligned}\right\} \tag{1}$$

where $u = f' = \partial f/\partial\eta$ is the x-component of velocity, $v = \eta f' - f - \xi\,\partial f/\partial\xi$ is the y-component of velocity, τ is the time, p is the pressure and f is the stream function. The parameters ρ_2 and ν_2 are for air; subscript 1 is for water.

These scales are introduced into the Navier–Stokes equations which are written below in the new dimensionless variables without approximation. The continuity equation becomes

$$\frac{\partial v}{\partial\eta} - \eta\frac{\partial u}{\partial\eta} + \xi\frac{\partial u}{\partial\xi} = 0. \tag{2}$$

The momentum equations are

$$\frac{\partial u}{\partial\tau} - \frac{\eta}{4\xi^2}u\frac{\partial u}{\partial\eta} + \frac{1}{4\xi}u\frac{\partial u}{\partial\xi} + \frac{1}{4\xi^2}v\frac{\partial u}{\partial\eta} = -\frac{1}{\rho}\left(-\frac{\eta}{4\xi^2}\frac{\partial p}{\partial\eta} + \frac{1}{4\xi}\frac{\partial p}{\partial\xi}\right)$$
$$+\nu\left(\left(\frac{1}{4\xi^2} + \frac{\eta^2}{16\xi^4}\right)\frac{\partial^2 u}{\partial\eta^2} + \frac{1}{16\xi^2}\frac{\partial^2 u}{\partial\xi^2} - \frac{\eta}{8\xi^3}\frac{\partial^2 u}{\partial\eta\,\partial\xi} + \frac{3\eta}{16\xi^4}\frac{\partial u}{\partial\eta} - \frac{1}{16\xi^3}\frac{\partial u}{\partial\xi}\right), \tag{3}$$

$$\frac{1}{\xi^2}\frac{\partial v}{\partial\tau} - \frac{\eta}{4\xi^4}u\frac{\partial v}{\partial\eta} + \frac{1}{4\xi^3}u\frac{\partial v}{\partial\xi} - \frac{uv}{4\xi^4} + \frac{1}{4\xi^4}v\frac{\partial v}{\partial\eta} = -\frac{1}{\rho}\frac{1}{\xi^2}\frac{\partial p}{\partial\eta}$$
$$+\nu\left(\left(\frac{1}{4\xi^4} + \frac{\eta^2}{16\xi^6}\right)\frac{\partial^2 v}{\partial\eta^2} + \frac{1}{16\xi^4}\frac{\partial^2 v}{\partial\xi^2} - \frac{\eta}{8\xi^5}\frac{\partial^2 v}{\partial\eta\,\partial\xi} + \frac{5\eta}{16\xi^6}\frac{\partial v}{\partial\eta} - \frac{3}{16\xi^5}\frac{\partial v}{\partial\xi} + \frac{3v}{16\xi^6}\right). \tag{4}$$

In the interface equations written below, $[.]$ designates the jump $(.)_1 - (.)_2$. At the interface $\eta = \eta^*(y = h(x))$, the velocity is continuous,

$$[u] = 0, \tag{5}$$

$$[v] = 0. \tag{6}$$

The shear stress is also continuous across $\eta = \eta^*$,

$$\left[\mu\left(\frac{1}{2\xi}\left(\frac{\eta^*}{\xi} + \frac{\partial\eta^*}{\partial\xi}\right)\frac{\partial v}{\partial\eta} + \frac{1}{2}\left(1 - \frac{1}{2}\left(\frac{\eta^*}{\xi} + \frac{\partial\eta^*}{\partial\xi}\right)\right)\left(\frac{\partial u}{\partial\eta} - \frac{1}{4\xi^2}v - \frac{\eta^*}{4\xi^2}\frac{\partial v}{\partial\eta} + \frac{1}{4\xi}\frac{\partial v}{\partial\xi}\right)\right)\right] = 0. \tag{7}$$

The jump in the normal stress is balanced by interfacial tension,

$$\left[p-\rho G\eta^*-2\mu\Big/\left(1+\left(\frac{\eta^*}{2\xi}+\frac{1}{2}\frac{\partial\eta^*}{\partial\xi}\right)^2\right)\left(\left(1-\left(\frac{\eta^*}{2\xi}+\frac{1}{2}\frac{\partial\eta^*}{\partial\xi}\right)^2\right)\frac{1}{4\xi^2}\frac{\partial v}{\partial\eta}\right.\right.$$
$$\left.\left.-\left(\frac{\eta^*}{2\xi}+\frac{1}{2}\frac{\partial\eta^*}{\partial\xi}\right)\left(\frac{1}{2\xi}\frac{\partial u}{\partial\eta}+\frac{1}{8\xi^2}\frac{\partial v}{\partial\xi}-\frac{\eta^*}{8\xi^3}\frac{\partial v}{\partial\eta}-\frac{1}{8\xi^3}v\right)\right)\right]$$
$$+S\Big/\left(1+\left(\frac{\eta^*}{2\xi}+\frac{1}{2}\frac{\partial\eta^*}{\partial\xi}\right)^2\right)^{3/2}\left(\frac{1}{8\xi}\frac{\partial^2\eta^*}{\partial\xi^2}+\frac{1}{8\xi^2}\frac{\partial\eta^*}{\partial\xi}-\frac{1}{8\xi^3}\eta^*\right)=0, \quad (8)$$

where $G=(g/U^2)(2\nu_2 x/U)^{1/2}$, g is the acceleration due to gravity, $S=T/(\nu_2\rho_2 U)$, and T is the coefficient of surface tension. We note here that in the above equations p is the dynamic pressure. Density and viscosity are normalized by the corresponding properties of the air

$$\rho=\begin{cases}\rho_1/\rho_2=815.6, & 0\leqslant\eta\leqslant\eta^*\\ 1, & \eta^*\leqslant\eta,\end{cases} \quad (9)$$

$$\mu=\begin{cases}\mu_1/\mu_2=64.01, & 0\leqslant\eta\leqslant\eta^*\\ 1, & \eta^*\leqslant\eta,\end{cases} \quad (10)$$

and $\nu=\mu/\rho$. The kinematic equation of the free surface is written in the boundary layer coordinates

$$\frac{4\xi}{u}\frac{\partial\eta^*}{\partial\tau}+\frac{\partial\eta^*}{\partial\xi}=\frac{1}{\xi}\left(\frac{v}{u}-\eta^*\right). \quad (11)$$

Equations (2)–(11) are a consistent non-dimensional set of equations which govern the flow in the air and the water. We note that the value the dimensionless kinematic viscosity takes in the water layer, $\nu=\nu_1/\nu_2$, is small, and the values that the non-dimensional density and non-dimensional viscosity take in the water layer are large. Our analysis however applies to any two fluids and does not make use of simplifications which might arise from small parameters. We have phrased the analysis in terms of air and water because we have aerodynamic applications in mind.

3. Non-similar boundary layers

We shall show later that the asymptotic solution for large ξ is similar, but not in the usual sense. We are motivated to see if this solution can be embedded in a large class of non-similar solutions for large ξ (large Reynolds number $Ux/2\nu_2$) and to investigate the possibility that the asymptotic solution enjoys a special status as a global attractor for all solutions of this non-similar family.

Self-similar boundary layers depend only on η and not on ξ. The ξ-derivatives of u, v and η^* may be small, of the order of $\xi^{-n}, n\geqslant 1$, when ξ is large. We retain those terms in each equation which are $O(1)$, dropping all terms of $O(\xi^{-n})$. For this computation we assumed that the first derivative of u with respect to ξ scales with ξ^{-1}, the second derivative with ξ^{-2} and $\partial\eta^*/\partial\xi$ with $\xi^{-3/2}$. These scalings can be verified in §6 *a posteriori*. We find that

$$ff''+\nu f'''-\xi\left(f'\frac{\partial f'}{\partial\xi}-f''\frac{\partial f}{\partial\xi}\right)=0 \quad (12)$$

holds in the air and water, and at $\eta=\eta^*$

$$\frac{\partial p}{\partial\eta}=0, \quad [f']=0, \quad [f]=0, \quad [\mu f'']=0, \quad [p]=[\rho]g\eta^*, \quad \frac{\partial\eta^*}{\partial\xi}=\frac{1}{\xi}\left(\frac{v}{u}-\eta^*\right). \quad (13)$$

Equation (12) can be found in Schlichting (1987, pp. 187–191). We may remark that the contributions of the viscous terms in the normal stress balance are ξ^{-2} times the terms retained and the surface tension terms are ξ^{-3} times those retained. We should emphasize that no thin layer assumption is made in this analysis. The results hold uniformly for all prescribed values of flux of water.

Equations (12) and (13) are valid approximations to the system given by (2)–(11) when ξ is large enough. We are at present preparing numerical simulations using the full Navier–Stokes equations to determine how large ξ must be in order for (12) and (13) to be valid.

4. Asymptotic solution for large ξ

Here we give a special solution of our coupled air–water system which will be shown later to be a global attractor of non-similar boundary layer solutions. This special solution is such that for large x (large ξ) the horizontal velocity component in the water is linear in y, the interface position $\eta^* \to 0$, and there is a similarity solution in the air with $f(0) = f'(0) = 0$, and $f''(0)$ is constant. In the air we write

$$u = f'(\eta), \quad \eta = ky/x^{1/2}, \tag{14}$$

and in the water

$$u = c(x)\,y, \quad Q = \int_0^h u\,\mathrm{d}y = \tfrac{1}{2}c(x)\,h^2 = \text{constant}. \tag{15}$$

We will show this solution is similar, i.e. satisfies the Blasius equation $ff'' + \nu f''' = 0$.

First we shall show that the continuity of the shear stress across the interface η^* implies that $c(x) = Ax^{-1/2}$, with A a constant, so that $u = A\eta$ can be expressed in terms of η alone. The interface is on $y = h(x), \eta = \eta^* = khx^{-1/2}$. The shear stress is continuous:

$$\mu_1 \frac{\partial u}{\partial y} = \mu_2 \frac{\partial u}{\partial y} \quad \text{at} \quad \eta^* = k\frac{h}{x^{1/2}}. \tag{16}$$

Hence

$$\mu_1\, c(x) = \mu_2 f''(\eta^*)\frac{\partial \eta}{\partial y} = \mu_2 \frac{k}{x^{1/2}} f''\left(\frac{kh}{x^{1/2}}\right). \tag{17}$$

In our solution $\eta^* = h(x)/x^{1/2} \to 0$, so that $f''(\eta^*) \to f''(0)$ which is constant and non-zero. Then

$$c(x) = \frac{\mu_2 k f''(0)}{\mu_1 x^{1/2}} = \frac{A}{x^{1/2}}. \tag{18}$$

Using (15), we may write

$$h^2 = \frac{2Q}{A}x^{1/2} \overset{\text{def}}{=} B^2 x^{1/2}, \tag{19}$$

$$h = Bx^{1/4}. \tag{20}$$

Using (20), we find that

$$\eta^* = \frac{kBx^{1/4}}{x^{1/2}} = \frac{kB}{x^{1/4}} \to 0, \tag{21}$$

which is consistent with our solution statement.

The boundary conditions at the wall, $\eta = 0$, and (21) imply that

$$f(\eta^*) \to f(0) = 0 \quad \text{as} \quad \xi \to \infty, \tag{22}$$

$$f'(\eta^*) \to f'(0) = 0 \quad \text{as} \quad \xi \to \infty. \tag{23}$$

The boundary conditions in the air have become the same as those for the Blasius solution for a boundary layer over a flat plate. Thus our initial solution in the air is realized, with $f''(\eta^*) \to f''(0) = \text{constant}$.

The flow in the water also satisfies the Blasius equation because the water layer in the non-dimensional coordinates is thin, $\eta^* \to 0$, even though the dimensional interface position $h(x) \to \infty$ as $x \to \infty$. The flow in the water may be described as a low Reynolds number flow, i.e. a local Reynolds number may be defined to be

$$\mathscr{R}_w = \frac{u(h(x))\, h(x)}{\mu_1} \approx \eta^{*2} \approx \frac{1}{\xi} \to 0. \tag{24}$$

Hence inertia effects are negligible. This is true even though the flow rate of water, Q, is a prescribed constant, and the inertia in the air is sensible.

5. Solutions of initial value problems for the non-similar two-fluid boundary layer equation

5.1. *Evolution of a profile which is initially parabolic in segments*

We now turn to numerical solutions of (12) and (13). Since the non-similar solutions depend on ξ, we are obliged to consider the evolution of flows prescribed at some initial position $\xi = \xi_0$, i.e. $f_0(\eta) = f(\eta, \xi = \xi_0)$, $\eta_0^* = \eta^*(\xi = \xi_0)$. Note that by fixing $f_0(\eta)$ and η_0^* we have fixed the flux of water $Q = (2\nu_2 xU)^{1/2} f(\eta^*)$, where by continuity Q is a constant which is prescribed. Fortunately our simulations of those initial value problems indicate a rapid decay from initial values to the asymptotic solution described in §4. This situation is not unfamiliar. In the classical theory of boundary layers, the Blasius solution (the similarity solution) is a global attractor for all initial value problems which are not similar (see Serrin 1967). In our case the attractor cannot be self-similar, but the non-similar solution of §4 arises asymptotically, for large ξ from all initial conditions explored. The first initial condition we used to solve (12) and (13) is plotted in figure 1. For this initial condition $\eta^* = 0.15$ and $\xi_0 = 50$. These values were chosen to be representative of conditions discussed by Hastings & Manuel (1985), in which they describe the results of their wind tunnel measurements of a wing in simulated rain. In the above profile, for $0 < \eta < \eta^*$, f' is parabolic with f''' being positive. For $\eta^* < \eta < 3.5$, f' is parabolic with f''' being negative. For $\eta > 3.5$, $f' = 1.0$.

We solved (12) and (13) subject to the above initial conditions for $\xi > \xi_0$ using a finite difference scheme found in Schlichting (1987, pp. 187–191). This scheme is iterative using second-order differencing for the η-derivatives, and a first-order implicit Euler differencing for the ξ-derivatives. In order to parametrize the interface shape which we calculated with the above method, we assumed an interface $\eta^* = a\xi^n$, where $a = \eta^*(\xi_0)/\xi_0^{n(\xi_0)}$, and found the $n(\xi)$ given in figure 2.

The exponent function $n(\xi)$ decays rapidly to $-1/2$, corresponding to a limiting power law $h(x) \propto x^{1/4}$ of the interface height as given by the asymptotic solution shown in figure 1. For ξ not much larger than ξ_0 the horizontal velocity component f' becomes linear in η, $f' = c(\xi)\,\eta$, in the water layer and remains so for all greater ξ. The shear stress in the water, $(\mu_1/\mu_2)\, c$, is directly related to the shear stress in the air at the interface through the tangential stress condition found in (13). From our calculations we find that the shear stress in the air at the interface, f'', asymptotically tends to the shear stress in the Blasius boundary layer of a single fluid over a flat plate at the plate surface, as shown in figure 3.

Notice that the exponent function $n(\xi)$ tends to its asymptotic value extremely

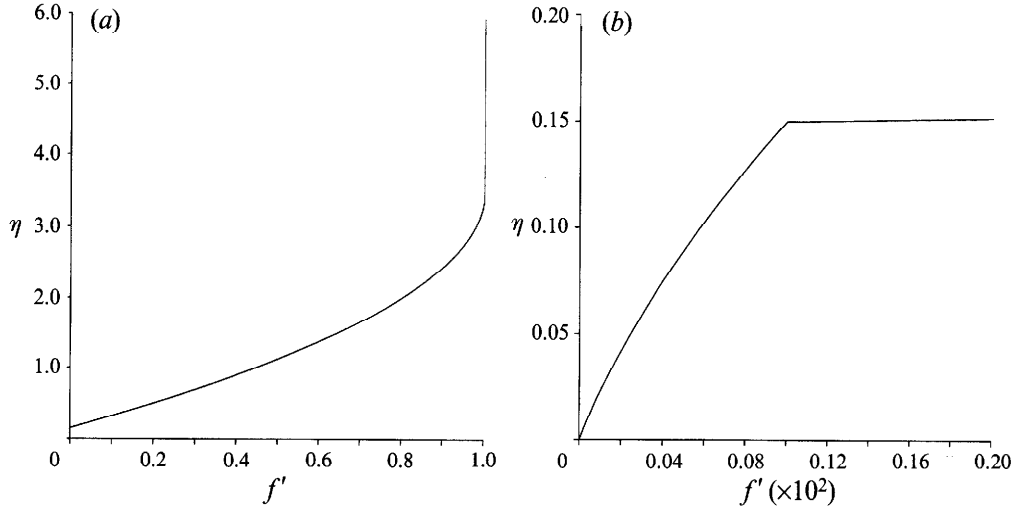

FIGURE 1. Parabolic initial condition assumed for the horizontal velocity component f' with $\eta^* = 0.15$ and $\xi_0 = 50$. (*a*) Initial condition. (*b*) Detailed plot of initial condition at the interface.

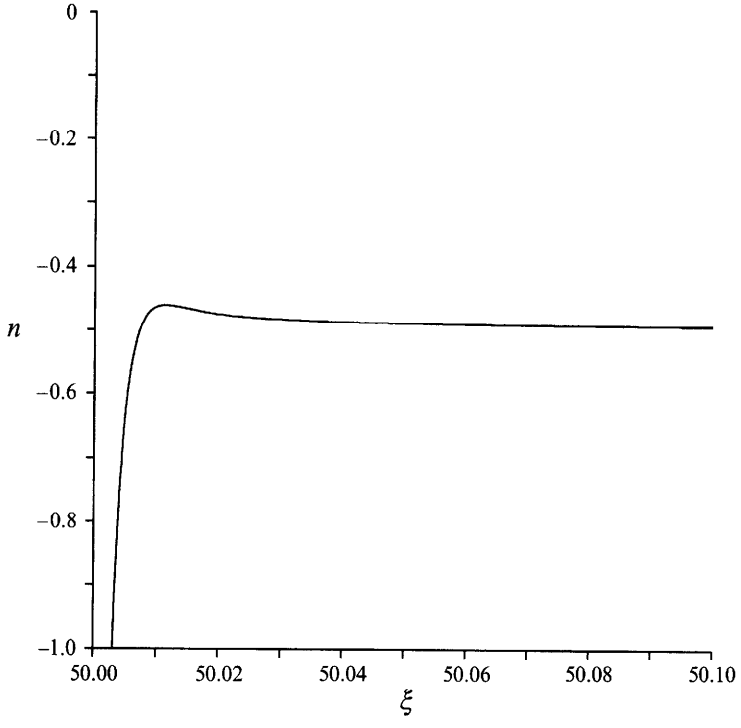

FIGURE 2. Plot of n for the non-similar boundary layer with initial conditions from figure 1.

rapidly, while the shear stress at the interface in the air f'' has a much slower decay. The reason for this difference is that the horizontal velocity component in the water becomes linear, and thus $n(\xi)$ becomes nearly $-1/2$, for ξ not very much greater than ξ_0. Figure 3 shows that the flow has not yet reached its asymptotic form, since the shear stress at the interface in the air is appreciably different from its asymptotic value. The flow then slowly tends to its asymptotic state. The flow is non-similar for finite ξ

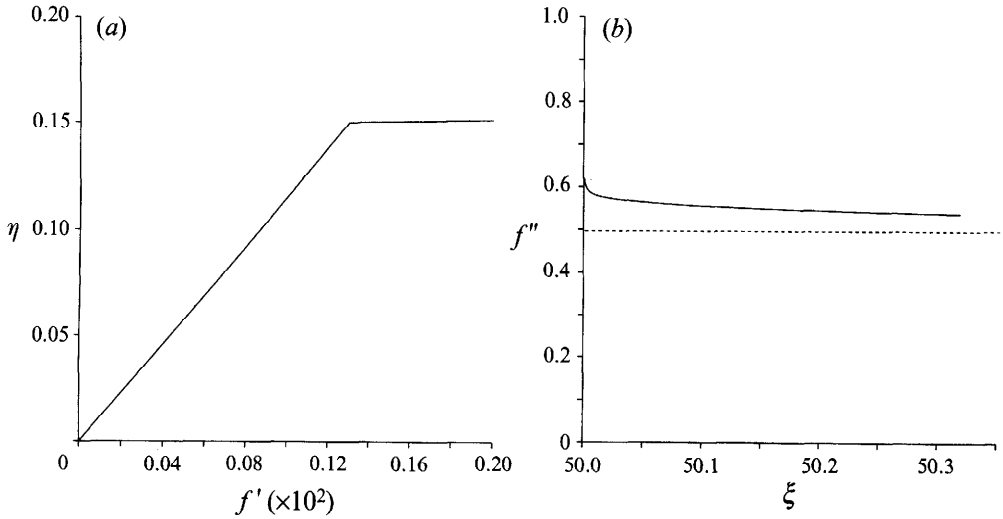

FIGURE 3. (*a*) Detailed plot of boundary layer solution in the water layer at $\xi = 50.0675$ for the initial conditions of figure 1. (*b*) Shear stress, f'', in the air at the interface, $\eta^* = a\xi^{n(\xi)}$, for $\xi > \xi_0$.

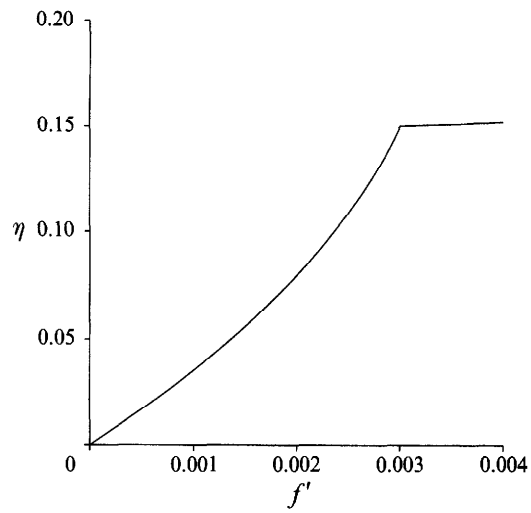

FIGURE 4. Initial profile in the water at $\xi = \xi_0$. The profile in the air is shown in figure 1(*a*).

because the boundary layer height and the interface do not scale the same. Asymptotically one may say that the flow is similar because η^* goes to zero and the flow in the air is the self-similar Blasius profile.

5.2. *Evolution of another profile which is initially parabolic in segments*

In the next example we used the same initial value for η^* and the same initial $f'(\eta)$ for $\eta > \eta^*$ as in figure 1(*a*), but the profile shown in figure 1(*b*) was replaced with the one shown in figure 4.

In figure 5 we show the evolution of the exponent $n(\xi)$ for $\xi > \xi_0$ for the above initial condition. Again $n(\xi) \to -1/2$ for large ξ and $\eta^* = a\xi^{-1/2}$ for large ξ. The solution given in §4 is attained asymptotically. Although not plotted here, $f''(\eta^*)$ again exhibits a slow relaxation to its asymptotic value.

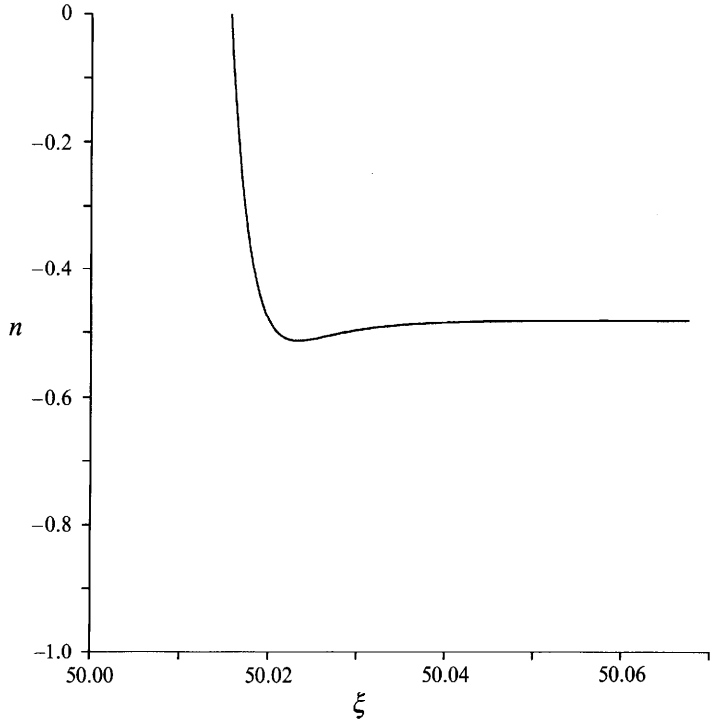

FIGURE 5. Exponent function $n(\xi)$ for $\eta^* = a\xi^{n(\xi)}$.

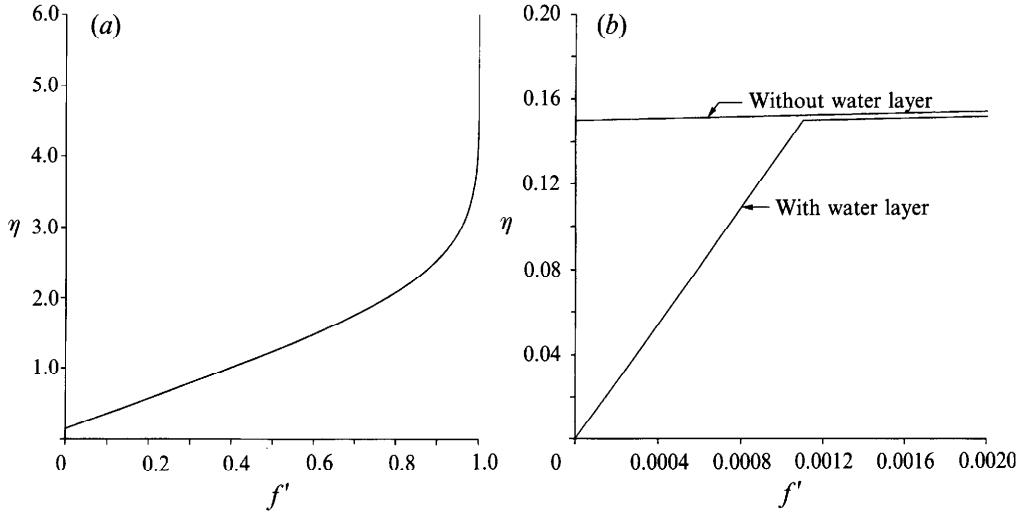

FIGURE 6. Solution $f'(\eta)$ of (25) and (26): (*a*) $\eta > 0.15$, (*b*) $\eta < 0.15$. The Blasius solution of (12) for $f(0.15) = f'(0.15) = 0$ is also shown in (*b*).

5.3. *Evolution of a profile which is initially in similarity form but with* $\eta^*(\xi_0) = 0.15 > 0$

The initial condition shown in figure 6 is generated from (12) and (13) when the ξ-derivatives are set to zero, so that

$$ff'' + \nu f''' = 0, \tag{25}$$

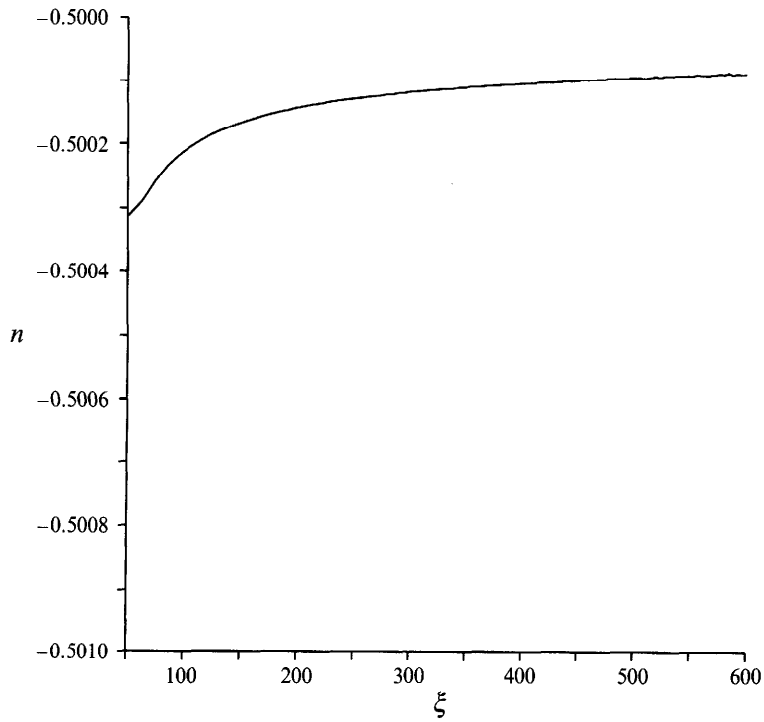

FIGURE 7. Exponent function $n(\xi)$ for $\eta^* = a\xi^{n(\xi)}$ for the initial conditions of figure 6.

and at $\eta = \eta^*$

$$\frac{\partial p}{\partial \eta} = 0, \quad [f'] = 0, \quad [f] = 0, \quad [\mu f''] = 0, \quad [p] = [\rho] g \eta^*. \tag{26}$$

In the following computations, the initial value of η^* was chosen to be the same as that given in figure 1 (*b*). This system is solved using an iterative finite difference scheme using second-order differencing and gives rise to the profiles shown in figure 6.

The profiles in figure 6 were used for initial values in the non-similar equations (12) and (13) and they evolved to the coupled self-similar solutions described in §4 in which $\eta^*(\xi) \to 0$. The difference between the solution in the air and the classical Blasius flat plate solution also tends to zero. A graph of the exponent function for this example is shown in figure 7.

In these examples and in all the others, which we tried but are not shown, the asymptotic solution given in §4 is ultimately attained.

6. Behaviour of ξ-derivatives of the non-similar solution

In deriving the system which lead to the above solutions, we assumed that first and second derivatives of u and η^* with respect to ξ were inversely proportional to ξ^{-n}, $n \geqslant 1$. From our solution we find that $\partial\eta^*/\partial\xi$ scales like $\xi^{-3/2}$ and $\partial^2\eta^*/\partial\xi^2$ scales like $\xi^{-5/2}$, in agreement with our scalings. Since ξ scales with $x^{1/2}$, the interface position scales with $x^{1/4}$.

In order to examine the ξ-derivatives of u, we define two functions:

$$F_1(\eta, \xi) = \xi\, \partial f'/\partial\xi, \tag{27}$$

$$F_2(\eta, \xi) = \xi^2\, \partial^2 f'/\partial\xi^2. \tag{28}$$

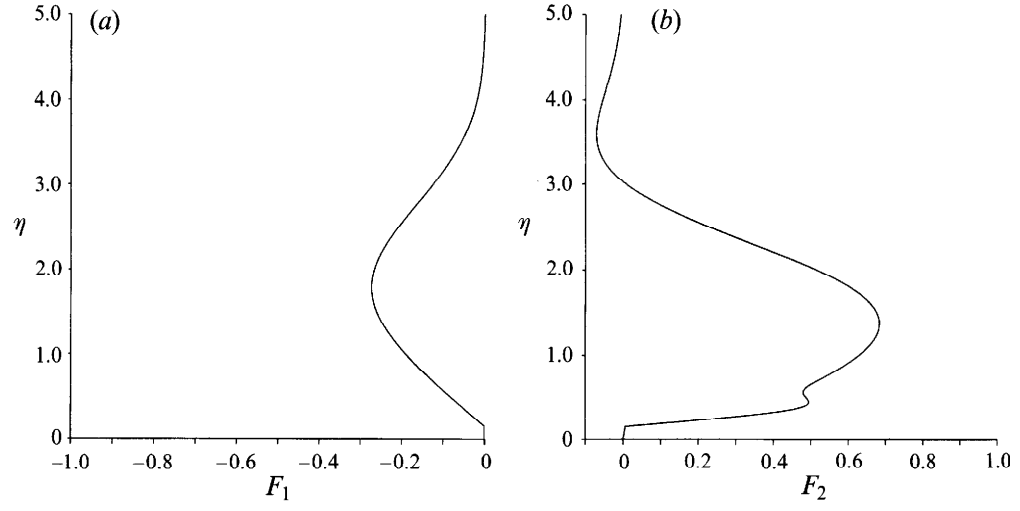

FIGURE 8. Plot of $F_1(\eta, \xi)$ and $F_2(\eta\xi)$ versus η for $\xi = 50.01$ for the flow plotted in figure 6.

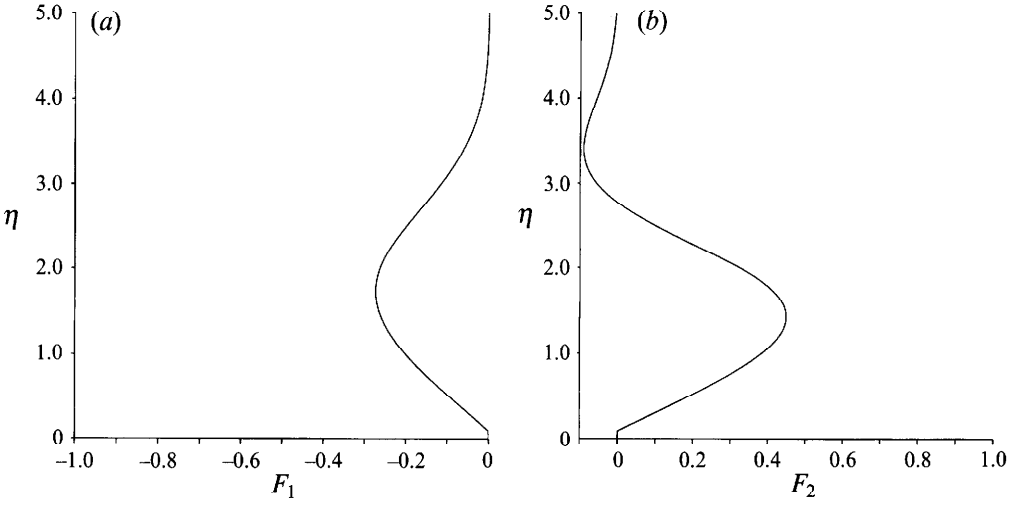

FIGURE 9. Plot of $F_1(\eta, \xi)$ and $F_2(\eta, \xi)$ versus η for $\xi = 129.1$ for the flow plotted in figure 6.

Depending upon the initial conditions chosen at ξ_0, $F_1(\eta, \xi_0)$ and $F_2(\eta, \xi_0)$ may be extremely large. However, for larger values of ξ the horizontal velocity component in the water becomes linear in η, $n(\xi)$ tends to $-1/2$ and $F_1(\eta, \xi) < 1, F_2(\eta, \xi) < 1$ (see figure 8). $|F_1|$ and $|F_2|$ decrease, as shown in figure 9, although the decrease in $|F_1|$ is very small. Then since F_1 and F_2 are both $O(1)$, the assumptions that were made in deriving (12) and (13) are shown to hold. Also, since as $\xi \to \infty, \eta^* \to 0$ and the flow in the air goes to the Blasius boundary, both $F_1 \to 0$ and $F_2 \to 0$ as $\xi \to \infty$.

7. Concluding remarks

The analysis given in this paper can be extended to two-fluid boundary layer problems with other free streams, say $U = U_\infty x^n$. It is also probable that the solution given in §4 and the other limiting solutions to which we have just alluded are unique

large-x limits of steady coupled air–water solutions of the Navier–Stokes equations with different initial profiles at $x = x_0$.

This work was supported by grants from NASA Langley, the National Science Foundation, the DOE, Department of Basic Energy Sciences, the US Army, Mathematics and AHPCRC, the Minnesota Supercomputer Center and the US Air Force, Wright Laboratories, Flight Dynamics Directorate. A large portion of this work was completed at the 1993 Workshop on Transition, Turbulence and Combustion hosted by NASA Langley Research Center's Institute for Computer Applications in Science and Engineering (ICASE).

REFERENCES

HASTINGS, E. C. JR. & MANUEL, G. S. 1985 Measurements of water film characteristics on airfoil surfaces from wind tunnel tests with simulated heavy rain. *AIAA Paper* 85-0259.

SERRIN, J. 1967 Asymptotic behaviour of velocity profiles in the Prandtl boundary layer theory. *Proc. R. Soc. Lond.* A **299**, 491–507.

SCHLICHTING, H. 1987 *Boundary-Layer Theory*, 7th edn. McGraw-Hill.

WANG, C. Y. 1992 The boundary layers due to shear flow over a still fluid. *Phys. Fluids* A **4**, 1304–1306.

YIH, C.-S. 1990 Wave formation on a liquid layer for de-icing airplane wings. *J. Fluid Mech.* **212**, 41–53.